

Digital Signal Processing for Fibre-Optical Parametrically Amplified Transmission Links

Long H. Nguyen, Sonia Boscolo, and Stylianos Sygletos

Aston Institute of Photonic Technologies, Aston University, Birmingham B4 7ET, United Kingdom

e-mail: {lnguy, s.a.boscolo, s.sygletos}@aston.ac.uk

ABSTRACT

We review our recent research progress on digital signal processing tailored for fibre-optical parametric amplifiers (FOPAs), by presenting an online method for correcting the accumulated amplitude and phase distortions induced by the phase modulation of the pump sources and its interaction with the dispersive fibre channel in transmission systems using cascaded FOPAs.

Keywords: Digital signal processing, fibre-optical parametric amplifiers, pump-phase modulation.

1. INTRODUCTION

Fibre-optical parametric amplifiers (FOPAs) relying on four-wave mixing to amplify the signals possess several advantageous properties for optical communications [1]. Nonetheless, stimulated Brillouin scattering (SBS) poses a major challenge to their integration into optical links because it limits the pump power that can be delivered to the highly nonlinear fibre (HNLF), hence the achievable signal gain [2]. A widely used approach to relax this limitation consists in broadening the pump-source linewidth via external phase modulation [3], e.g, using a combination of radiofrequency (RF) tones. While pump-phase modulation is a very effective SBS mitigation technique [4], it introduces temporal fluctuations in the complex parametric gain through the modulation of the instantaneous pump frequency [5], which affect the phase and amplitude of the amplified signals. Moreover, the interaction of the induced phase distortion with the fibre chromatic dispersion in a transmission link results in a phase-to-amplitude distortion transfer [6], which becomes more severe with increasing transmission distance along the link because of the extended channel memory.

Addressing SBS at the device level has shown promise [7], but it tends to increase device complexity and cost. Alternatively, digital signal processing (DSP) has a proven ability to resolve performance issues in commercial systems, thereby indicating that DSP tailored for FOPAs could offer a viable solution for their broader adoption in optical networks. Our recent research has developed various DSP techniques to mitigate the impact of pump dithering in fibre-optical parametric devices [8]-[10]. Particularly, in [9] we have introduced a fully online algorithm capable of effectively reconstructing and eliminating from the received signal the phase and amplitude distortions accumulated along a transmission link with cascaded FOPAs, operating with a multi-tone pump-phase modulation to achieve the necessary SBS-limited gain. Here, we review these results and further illustrate our dithering-induced distortion compensation (DDC) method when used with dual-pump FOPA schemes in the realistic scenario of imperfect counter-phase modulation of the pumps.

2. METHODS

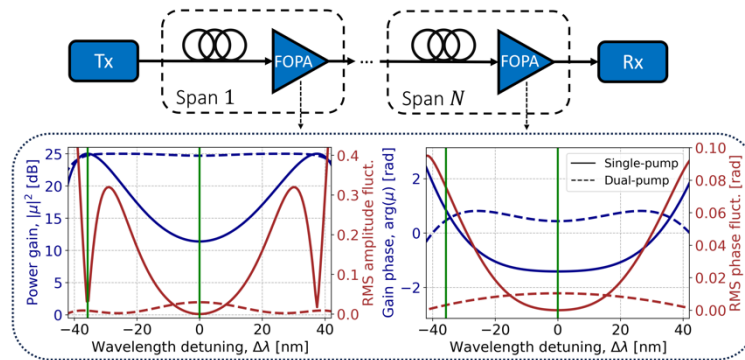


Figure 1. Schematic diagram of a transmission system with N cascaded FOPA stages. The inset shows the power and phase spectral responses of the gain of single- and dual-pump FOPAs versus wavelength detuning from the pumps, and the dithering-induced RMS fluctuations of the gain's amplitude and phase. The green vertical lines indicate the operating points for the performance evaluation of the DDC method.

We considered an optical fibre transmission system comprising N identical spans, each of 100-km standard single-mode fibre followed by a FOPA to compensate the span losses (Fig. 1(a)). We modelled the FOPA by its complex signal gain, which in the absence of pump depletion is given by [1] $\mu(t) = \{\cosh(g(t)L) + i[\kappa(t)/(2g(t))]\sinh(g(t)L)\}e^{i[2\gamma P - \kappa(t)/2]L}$, where L is the effective fibre length, $P = P_1 + P_2$ is the total pump

power, γ is the nonlinear coefficient of the fibre, $g(t) = \sqrt{(\gamma P)^2 - (\kappa(t)/2)^2}$ is the parametric gain coefficient, and $\kappa(t)$ is the phase mismatch, comprising an instantaneous term driven by the first derivative $\dot{\varphi}_t$ of the pump-phase modulation $\varphi(t) = \varphi_1(t) + \varphi_2(t)$ [5]. In the case when the two pumps are modulated in opposition of phase, φ represents the unavoidable residual phase modulation due to the practical difficulty of adjusting the delays and phases of the electrical signals driving the phase modulators [12]. The maximum FOPA's power gain was set to $20\log(\cosh(\gamma PL)) = 25$ dB, accounting for an additional insertion loss of the device. The inset of Fig. 1 shows typical examples of the power and phase spectral responses of the parametric gain as a function of the signal detuning $\Delta\lambda$ from the mean pump wavelength in the absence of pump-phase modulation, and the root-mean-square (RMS) fluctuations of the gain's amplitude and phase caused by a four-tone phase modulation. In the single-pump FOPA case, the phase fluctuation features a fast growth with increasing detuning from the pump and represents the primary source of signal distortion when the FOPA is operated at the signal detuning of maximum gain where the amplitude fluctuation is negligibly small. The nearly uniform gain in the spectral region between the two pumps enables broadband operation of the dual-pump FOPA. Interestingly, the gain's amplitude and phase fluctuations show opposite dependence on $\Delta\lambda$ to the single-pump case. For illustration purposes, we operated the amplifier at the same detuning as its single-pump counterpart ($\Delta\lambda = 35.7$ nm) and at $\Delta\lambda = 0$.

Reaching an SBS-limited gain level of 25 dB requires an enhancement of the Brillouin power threshold by a factor between 12 and 18 for a range of HNLFs in the 1550-nm region [2]. To achieve this, we considered a multi-tone modulation of the pump phase, $\varphi_1(t) = \sum_{j=1}^{N_t} A_{m_j} \sin(\omega_{m_j} t + \xi_{m_j})$, where the base frequency ν_{m_1} was set to a larger value than the Brillouin bandwidth for typical HNLF ($\nu_{m_1} = 60$ MHz), and we selected a multiple of three spacing between successive tones to maximise the pump spectral broadening and power distribution [3]. The tone's amplitudes A_{m_j} and phases ξ_{m_j} were optimised to ensure a nearly uniform power distribution among the 3^{N_t} peaks generated across the broadened pump spectrum by using stochastic gradient descent in TensorFlow [9]. The imperfect pump counter-phase modulation in the dual-pump FOPA was accounted for in our model by amplitude and phase mismatches between the phase-modulation waveforms of the two pumps [8], i.e., we used $\varphi_2(t) = -\sum_{j=1}^{N_t} (A_{m_j} + \delta A_m) \sin(\omega_{m_j} t + \xi_{m_j} + \delta \xi_m)$ for the second pump.

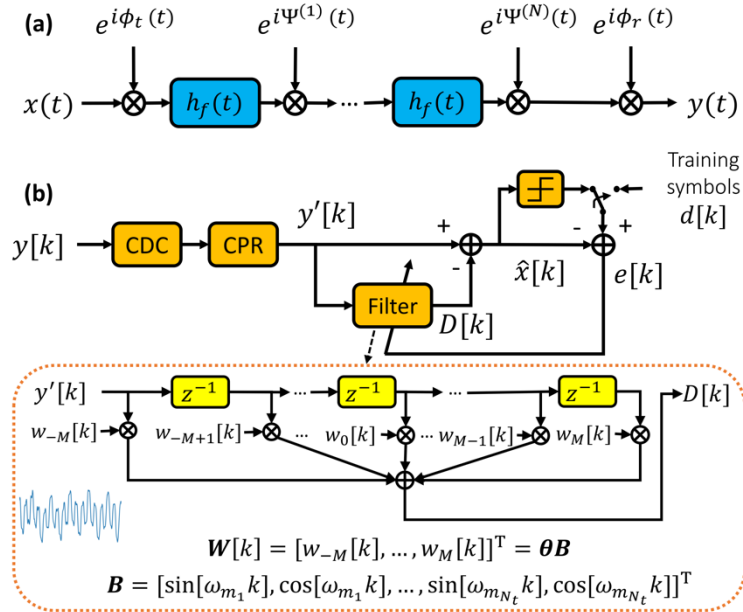


Figure 2. (a) Baseband equivalent of the FOPA link shown in Fig. 1. (b) Block diagram of the DDC-enabled DSP chain. The inset shows the principle of the DDC algorithm.

To correct the signal distortion at the receiver, we reverse engineered the transmission link, focusing on how the phase fluctuation of the FOPA's gain caused by pump dithering interacts with the fibre dispersion. Hence, we assumed the equivalent baseband model of Fig. 2(a), where $h_f(t)$ represents the linear impulse response of each fibre span, $\phi_t(t)$ and $\phi_r(t)$ are the Wiener random phase noises (PNs) of the transmitter and receiver laser sources, respectively, $\Psi^{(n)}(t) = \phi_p^{(n)}(t) + \phi^{(n)}(t)$ is the total phase distortion introduced at the n^{th} FOPA stage, $\phi_p^{(n)}(t)$ is the pump laser PN, and $\phi^{(n)}(t)$ represents the dithering-induced phase fluctuation of the FOPA's gain. By applying linear backpropagation to the relationship between input $x(t)$ and output $y(t)$ signal waveforms, we derived an approximate estimate of the transmitted signal $\hat{x}(t)$. This equation evidenced that the output signal from a conventional DSP chain including chromatic dispersion compensation (CDC) and carrier phase recovery

(CPR) (Fig. 2(b)), $y'(t) = e^{-i\delta\phi(t)}[y(t) * h_e^{(N)}(t)]$ (where $\delta\phi(t) = \sum_n \phi_p^{(n)}(t) + \phi_t(t) + \phi_r(t)$, and $h_e(t)$ is the inverse response of the fibre span, and the superscript (N) refers to the accumulation by N spans), differs from the transmitted signal by an additional dithering-dependent complex distortion term, which becomes more important with increasing number of fibre spans. By approximating the channel impulse response by a finite impulse response filter, this distortion term at the time instance k can be written as $D[k] = i \sum_{m,m'=-M/2}^{M/2} y'[k - m - m'] \sum_{n=1}^N (h_{f,m}^{(n)} \phi^{(n)}[k - m'] h_{e,m'}^{(n)})$, where $M/2$ is the filter delay corresponding to the channel memory of the N -span link. This equation shows that we can recreate $D[k]$ by passing $y'[k]$ through an adaptive digital filter whose taps have similar form to the first-order time derivative of the pump phase ϕ_t (inset of Fig. 2(b)) and, thus, can be predicted by fitting a parametric model with the known pump phase modulation frequencies used at each FOPA stage. Therefore, by using the complex least-mean-square algorithm [11], we fitted a time-varying filter $\mathbf{W}[k] = [w_{-M}[k], \dots, w_M[k]]^T$ such that $D[k] = \mathbf{W}^T[k] \mathbf{Y}'[k]$, where $\mathbf{Y}'[k]$ represents the signal block after the conventional CDC and CPR stages. The filter was trained by updating the coefficient vector $\boldsymbol{\theta}$ in the linear regression form $\mathbf{W} = \boldsymbol{\theta} \mathbf{B}$, where the feature vector was defined as $\mathbf{B}[k] = [\sin[\omega_{m_1} k], \cos[\omega_{m_1} k], \dots, \sin[\omega_{m_{N_t}} k], \cos[\omega_{m_{N_t}} k]]^T$. The transmitted signal at time k was then recovered as $\hat{x}[k] = y'[k] - \mathbf{B}^T \boldsymbol{\theta}^T[k] \mathbf{Y}'[k]$. The update of $\boldsymbol{\theta}$ was made at the symbol rate using the error calculated from the estimated symbol and the reference one, where the reference symbol was given from the decision-directed operation when the algorithm exited the training phase. In each cycle, the algorithm requires $4MN_t + 1$ and $M(2N_t + 1)$ multiplication operations to update $\boldsymbol{\theta}$ and produce the recovered symbol $\hat{x}[k]$, respectively.

3. RESULTS AND DISCUSSION

We performed numerical simulations of the transmission of a single-polarisation 16 quadrature-amplitude modulation (QAM) Nyquist shaped signal at 28-Gbaud rate over a channel consisting of $N=12$ fibre spans. The laser linewidths were 50 kHz and 30 kHz for the transmitter and receiver units and the FOPA pumps, respectively. To avoid the signal symbols experiencing the same distortions along the FOPA link, we included a random time shift in the pump-phase modulation sinusoidal waveforms at each FOPA stage. Similarly, in the dual-pump case, the amplitude and phase mismatches δA_m and $\delta \xi_m$ were sampled at each FOPA stage from normal distributions with zero mean and standard deviations 0.5 and 0.35 rad, respectively. The amplifier's noise figure was 4.5 dB, and the Q^2 -factor derived from the directly counted bit-error-rate (BER) on a total number of 10×2^{16} symbols was used as a system's performance metric.

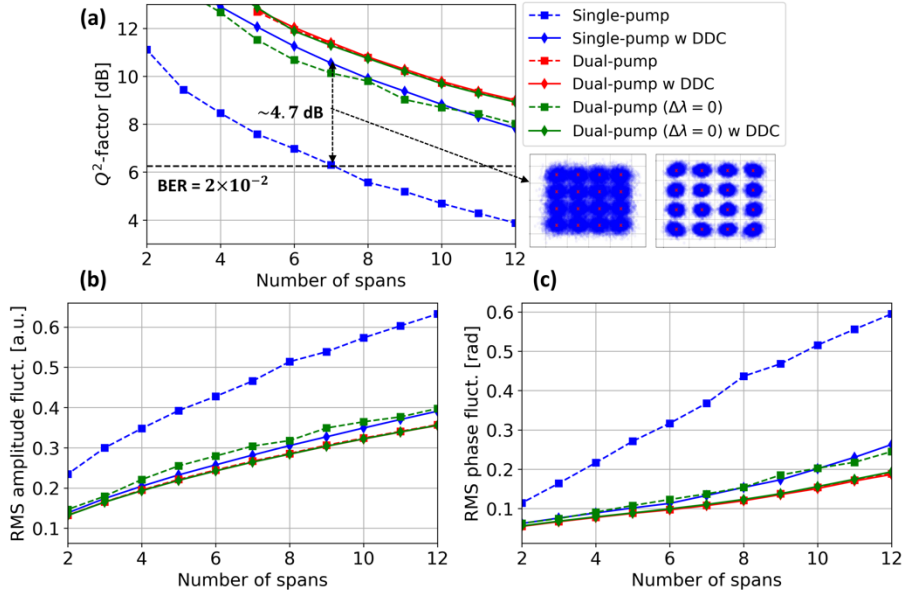


Figure 3. (a) Q^2 -factor after conventional (CDC+CPR) (dashed) and DDC-enabled (solid) DSP versus number of fibre spans for in-line amplification by single-pump FOPAs (blue), and dual-pump FOPAs operated at the edges (red) and the centre (green) of the gain's bandwidth. The inset shows the signal constellations for in-line single-pump FOPAs without and with DDC after seven spans. (b,c) Evolution of the root-mean-square phase and amplitude fluctuations after conventional and DDC-enabled DSP over number of fibre spans.

Figure 3(a) shows the performance of our developed DDC algorithm as a function of the transmission length, for the single- and dual-pump FOPA configurations using a four-tone pump-phase modulation. For comparison, we also included the performance curves recorded after the CPR stage, which was implemented by using the feedforward blind phase search (BPS) method [13]. The launched signal power and lengths of the BPS filter block

and DDC filter were optimised at the maximum transmission length considered. In the single-pump FOPA case, our DDC method brings about significant performance benefits across a wide range of transmission lengths, achieving approximately 4.7-dB improvement in Q^2 -factor over conventional DSP at a BER level of 2×10^{-2} , reached after 700-km transmission. The capability of the DDC method to mitigate both phase and amplitude signal distortions accrued along the transmission link is corroborated by Figs. 3(b) and 3(c), showing the evolution over the transmission length of the RMS deviations of the phases and amplitudes, respectively, of the received symbols compared to the transmitted ones, after post-processing by the conventional and DDC-enhanced DSP chains. On the contrary, when dual-pump FOPAs operated near the band edges of their gain spectrum are deployed in the transmission link, there is no apparent benefit in using our DDC method as the impact of an imperfect pump counter-phase modulation on the amplifier's gain, hence the amplified signal, is negligible (Fig. 1). Nevertheless, for a FOPA's operation around the centre of the gain bandwidth where the gain's fluctuations are no longer negligible, our DDC algorithm achieves around 1-dB Q^2 -factor improvement over conventional DSP. This indicates that the algorithm can be advantageously deployed in wavelength-division multiplexing transmission scenarios.

4. CONCLUSIONS

We have discussed the design of suitable DSP for transmission links using cascaded FOPAs. We have presented an online algorithm that, when added at the end of a conventional DSP chain, effectively reconstructs the accumulated amplitude and phase distortions originating from the pump-phase modulation and its interaction with the fibre dispersion, and then eliminates them from the received signal. Our current research is focused on the development of compensation techniques based on complex-valued kernels, which function as single-stage online equalisers handling both amplitude and phase distortions from pump dithering and random PN from laser sources, without needing prior knowledge of the dithering frequencies [14]. This research avenue holds great promise for the practical deployment of FOPAs in optical communication systems.

ACKNOWLEDGEMENTS

This work was supported by the H2020 MSCA ETN project POST-DIGITAL (EC 263 GA 860360), UK EPSRC grants TRANSNET (EP/R035342/1) and CREATE (EP/X019241/1), and NATO grant MELITE (G6137).

REFERENCES

- [1] M. Marhic: *Fiber Optical Parametric Amplifiers, Oscillators and Related Devices*, Cambridge University Press, Cambridge, UK, 2007.
- [2] V. Gordienko, *et al.*: Limits of broadband fiber optic parametric devices due to stimulated Brillouin scattering, *Opt. Fiber Technol.*, vol. 66, pp. 102646, 2021.
- [3] J.B. Coles, *et al.*: Bandwidth-efficient phase modulation techniques for stimulated Brillouin scattering suppression in fiber optic parametric amplifiers, *Opt. Express*, vol. 18, pp. 18138-18150, 2010.
- [4] T. Torounidis, P.A. Andrekson, and B.-E. Olsson: Fiber-optical parametric amplifier with 70-dB gain, *IEEE Photon. Technol. Lett.*, vol. 18, pp. 1194-1196, 2006.
- [5] A. Mussot, *et al.*: Impact of pump phase modulation on the gain of fiber optical parametric amplifier, *IEEE Photon. Technol. Lett.*, vol. 16, pp. 1289-1291, 2004.
- [6] J. Wang and K. Petermann: Small signal analysis for dispersive optical fiber communication systems, *J. Lightwave Technol.*, vol. 10, pp. 96-100, 1992.
- [7] M. Bastamova, *et al.*: Impact of pump phase modulation on QAM signals in polarization-insensitive fiber optical parametric amplifiers, *Opt. Fiber Technol.*, vol. 84, pp. 103758, 2024.
- [8] S. Boscolo, *et al.*: Kernel adaptive filtering-based phase noise compensation for pilot-free optical phase conjugated coherent systems, *Opt. Express*, vol. 30, pp. 19479-19493, 2022.
- [9] L.H. Nguyen, S. Boscolo, and S. Sygletos: Online digital compensation of pump dithering induced phase and amplitude distortions in transmission links with cascaded fibre-optical parametric amplifiers, *Opt. Express*, vol. 32, pp. 13467-13477, 2024.
- [10] L.H. Nguyen, S. Boscolo, and S. Sygletos: Online kernel-based phase recovery for parametrically amplified optical transmission, in *CSNDSP 2024*, Rome, Italy, Jul. 2024, Accepted.
- [11] B. Widrow, J.M. McCool, and M. Ball: The complex LMS algorithm, in *Proc. of the IEEE*, vol. 63, pp. 719-720, 1975.
- [12] M.A.Z. Al-Khateeb, *et al.*: Experimental demonstration of 72% reach enhancement of 3.6 tbps optical transmission system using mid-link optical phase conjugation," *Opt. Express*, vol. 26, pp. 23960-23968, 2018.
- [13] T. Pfau, S. Hoffmann, and R. Noe: Hardware-efficient coherent digital receiver concept with feedforward carrier recovery for M-QAM constellations, *J. Lightwave Technol.*, vol. 27, pp. 989-999, 2009.
- [14] L.H. Long, S. Boscolo, and S. Sygletos: Complex-valued kernel-based phase and amplitude distortion compensation in parametrically amplified optical links, 2024, Submitted.